Synthesis of Magnetic Novel Hybrid Nanocomposite (Fe₃O₄@SiO₂/Activated Carbon) by a Green Method and Evaluation of Its Antibacterial Potential

Fekri, Mohammad Hossein*⁺; Tousi, Fatemeh
Department of Chemistry, Ayatollah Borujerdi University, Borujerd, I.R. IRAN

Heydari, Rouhollah
*Research Center for Environmental Determinants of Health, Health Institute,
Kermanshah University of Medical Sciences, Kermanshah, I.R. IRAN*

Razavi Mehr, Maryam
Department of Chemistry, Ayatollah Borujerdi University, Borujerd, I.R. IRAN

Rashidipour, Marzieh
Nutritional Health Research Center, Lorestan University of Medical Sciences, Khorramabad, I.R. IRAN

ABSTRACT: *Inorganic antibacterial nanoagents have more advantages compared to popularly organic agents due to chemical stability, thermal resistance, immunity, and long-term activity. In this study, a magnetically hybrid nanocomposite was prepared from the Nigella sativa oil waste as an organic matrix in a green approach. The homogeneous distribution of core-shell Fe₃O₄@SiO₂ nanoparticles on the activated carbon surface was carried out with a simple chemical method. Characterization of the synthesized nanocomposite was performed by different analysis techniques such as scanning electron microscopy–energy dispersive spectroscopy, scanning electron microscopy, X-ray diffraction, and Brunauer-Emmett-Teller surface area analysis. The antibacterial activities of the prepared nanoparticles against gram-positive and gram-negative bacteria were investigated and the minimum inhibitory concentration and the minimum bactericidal concentration values were compared to imipenem as a standard antibiotic. The effects of temperature, time, and the ratio of the activated carbon to Fe₃O₄@SiO₂ on the MIC and MBC values of the prepared nanocomposites were investigated. The obtained results reveal the substantial role of all of these parameters in the gram-positive antibacterial potential, especially for S. agalactiae bacteria. The results show that the new proposed nanocomposite could be an alternative for an effective filter against gram-positive bacteria alongside having magnetic properties.*

KEYWORDS: *Magnetically hybrid nanocomposite; Nigella sativa; Activated carbon; Antibacterial Potential.*

INTRODUCTION

Consumption of contaminated water, whether for drinking or agricultural purposes, causes increased morbidity and mortality from infectious diseases and the matter has become a great concern. On the other hand, continuous development and synthesis of novel antimicrobial compounds have increased antimicrobial-resistant pathogenic microbes. In this effort, nanomaterials have fascinated a great deal of attention because of their unrivaled physical and chemical properties [1-3]. To date, many antimicrobial nanomaterials have been reported to be associated with toxicity, environmental pollution, biological incompatibility, and complex synthesis methods [4, 5]. Reckoning with this fact, the production of efficient, novel, and environmentally friendly antibacterial nanomaterials is an important challenge.

Organic compounds, as one of the most commonly used disinfectants for water asepsis, have some detriments, containing toxicity to human organs. Synthesis and development of biocompatible mineral disinfectants such as metal oxide nanoparticles are widespread among many research groups [6]. Inorganic nanocomposites containing $Fe_3O_4@SiO_2$ nanospheres are a notable candidate for a new magnetic disinfectant. These materials are environmentally friendly in addition to the simple methods and equipment required for their preparation [7-9]. Fe_3O_4 magnetic nanoparticles are easily recoverable and reusable due to their superparamagnetic and heterogeneous phase properties. Silica has been used as a coating material for magnetic nanoparticles and forms core-shell $Fe_3O_4@SiO_2$ microspheres. The silica layers are coated on magnetic nanospheres with a smooth surface [10, 11] and often static silica coating on the surface of magnetic nanoparticles prevents their agglomeration in the liquid improving their chemical stability and providing better protection against toxicity [12]. In addition, silica layers efficiently protect the magnetite core against corrosion and oxidation due to their unique surface chemistry [13].

The use of Activated Carbon (AC) has demonstrated numerous advantages such as wide surface area, pore structure, high adsorption capacity, reactivity, and low cost compared to other adsorbents. In recent years, AC production from agricultural waste has increased mainly because of its low cost and availability [14-17]. Due to economic and environmental reasons, the interest in the development of efficient and sustainable composites has been rising

for chemists and material scientists [18]. So far, a number of composites containing AC have been prepared and often used as adsorbents for aquatic environmental pollutants [19- 22].

Gram-positive bacteria are of particular importance compared with gram-negative bacteria, since they are more stable and resistant, especially in aquatic environments (sea and lake) [23]. In order to determine the sensitivity of each microorganism against each antimicrobial agent, it is necessary to determine the diameter of the halo, the Minimum Inhibitory Concentration (MIC), and the Minimum Bactericidal Concentration (MBC). Nanomaterials are increasingly used to target bacteria as superior to antibiotics. This is due to the fact that antibiotics kill only a very small number of causative agents while nanomaterials destroy about 650 types of causative agents [24]. In nanomaterials laboratory tests, bacteria, viruses, and fungi are destroyed within minutes after contact with the nanoparticles [25]. The precise mechanism of nanoparticle toxicity to different bacteria is not entirely understood. This phenomenon is most likely related to electrostatic and/or hydrophobic interactions between bacteria membranes and nanoparticles which interrupt the entirety of the bacterial membrane. The effectiveness of nanoparticle toxicity depends on the combination, surface adjustment, inherent properties, and bacterial types. However, nanoparticles are able to directly influence the growth and proliferation of bacteria because of their high membrane permeability [26].

Due to the antibacterial property of *Nigella sativa* extract, the presence of the AC antibacterial effect of *Nigella sativa* oil waste is likely. Therefore, in this study, it was used as a crude material for the production of AC as a suitable substrate for nanocomposite preparation. *Nigella sativa* is known as a natural antioxidant that stops or delays the oxidation process [27].

Through this research, $Fe_3O_4@SiO_2/AC$ nanocomposite was synthesized and its potential for the growth rate inhibition of two gram-positive, *S. epidermidis* and *S. agalactiae*, and two gram-negative, *K.pneumonia* and *S.typhi*, bacteria were studied. Up to now, $Fe_3O_4@SiO_2/AC$ nanocomposite has not been reported as an antibacterial material. Since this is an entirely new field, scant studies have been conducted on the safety, noxiousness, and impact of nanoparticles, especially over long periods. It is then necessary to analyze possible effects on living

organisms and to investigate the effect of the over-use of nanoparticles in locally contaminated water. Finally, it should be mentioned that this Novel Hybrid Nanocomposite as a green composite and magnetic antibacterial nano filter is a material with nature-friendly properties which is technically and economically cost-effective.

In most previous studies, the inhibitor separation is carried out by filtration and centrifugation methods. These methods have mainly developed additional costs. On the other hand, these techniques may not be able to completely isolate the inhibitor from the sample, and instead result in the formation of secondary turbidity. To overcome the problems described, a magnetized activated carbon is suggested as an appropriate solution. In this method, the modification of activated carbon with iron oxide as a magnetic source is used for quick and easy separation of inhibitors by an external magnetic field. The regeneration ability of the magnetic inhibitors represents that these green technologies can be applied to full-scale wastewater treatment (industrial application) many times, as well as batch-inhibitor tests.

EXPERIMENTAL SECTION
Materials and Apparatus

Muller Hinton Agar medium, Muller Hinton Broth medium, 2, 3, 5-triphenyltetrazolium chloride, tetraethyl orthosilicate (TEOS), $FeCl_3.6H_2O$, $FeCl_2.4H_2O$, and all used solvents were purchased from the Merck Chemical Co. (Darmstadt, Germany). The gram-positive bacteria including *Staphylococcus* (1435: PTCC *S. epidermidis*), *Streptococcus* (*1768: PTCC S. agalactiae*), and the gram-negative bacteria of *Celysella* (1290: PTCC *K. pneumonia*) and *Salmonella* (1609: PTCC *S. typhi*) were obtained from the Persian Type Culture Collection (PTCC).

X-Ray Diffraction (XRD) patterns were recorded by a Shimadzu X-6000 instrument at 40 kV using Cu K_α (λ= 0.154 nm) radiation. SEM and EDX images were obtained using a Cambridge S-360 apparatus. The results of Brunauer-Emmett-Teller (BET) surface area analysis were obtained by a surface area analyzer (Quantachrome AS1Win).

Preparation of Activated Carbon (AC)

The activated carbon was synthesized using *Nigella sativa* oil waste as a precursor. The precursor was purchased from local stores in Borujerd city (Iran). First, the appropriate amount of the raw material was weighed

and washed with distilled water. Then it was dried in the oven at the temperature of 110 °C for 4 hours. The dried materials were grounded and sieved two times (particles with diameters less than 100 μm were collected). After that, 10 g of the dried materials were transferred into a crucible and placed in the oven at the temperature of 500 °C for three hours. Then, the sample was cooled to 25 °C, and the resulting powder was transferred into an Erlenmeyer flask. The powder was immersed in nitric acid with a purity of 65% at the temperature of 40 °C for three hours under vigorous stirring. The sample was left for one day in the same situation. Finally, the sample was dried in the oven at the temperature of 110 °C for two hours and Activated Carbon (AC) was produced.

Synthesis of Fe₃O₄ nanoparticles

Fe_3O_4 nanoparticles were prepared through the stopper method [28, 29] with minor modifications. Briefly, 0.994 g of $FeCl_2.4H_2O$ and 2.702 g of $FeCl_3.6H_2O$ were dissolved in 10 mL of deionized water. The mixture was transferred into a three-necked flask and stirred for three hours at a certain temperature under a nitrogen atmosphere. Then, under vigorous mechanical stirring 20 mL of concentrated ammonia was added to the flask. The final pH value of the mixture was reached around 9. The black precipitate was separated from the reaction medium under a magnetic field and washed 3 times with ethanol 96%. Finally, the black powder was dried in the oven at 65 °C for 18 hours (Eq. (1)).

$$2Fe(III) + Fe(II) + 8OH^- \rightarrow \qquad (1)$$

$$Fe(OH)_2 + 2Fe(OH)_3 \rightarrow Fe_3O_4 + 4H_2O$$
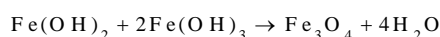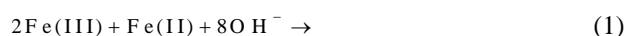
Synthesis of Fe₃O₄@SiO₂ nanoparticles

In a typical reaction, 0.1g of obtaining Fe_3O_4 nanoparticles, 40 mL ethanol, 10 mL deionized water, and 6 mL of concentrated ammonia were mixed in a three-necked flask followed by mild stirring for one hour at room temperature under an N_2 atmosphere. Then, 1 mL of tetraethoxysilane (TEOS) was added drop by drop into the flask followed by vigorous stirring for one hour under an N_2 atmosphere. Finally, obtained $Fe_3O_4@SiO_2$ nanoparticles were separated by a magnet and stored in a sample container until required.

Preparation of Fe₃O₄@SiO₂/AC nanocomposite

$Fe_3O_4@SiO_2/AC$ nanocomposite was prepared according to the following procedure: First, a certain

amount of activated carbon was added to the beaker and dispersed in ethanol (5 mL) by an ultrasonic bath for 5 minutes. Subsequently, a certain amount of $Fe_3O_4@SiO_2$ was gradually added to the activated carbon at a ratio of (6:1, 4:1, and 2:1) and more dispersed in an ultrasonic bath for 5 minutes. Finally, the mixture was stirred at the desired temperatures (30, 40, and 50) °C for a specified period of 8, 16, and 24 hours. The influence of various temperatures 30, 40, and 50 °C on the antibacterial property of $Fe_3O_4@SiO_2/AC$ nanocomposite was surveyed. The selected values of time and the ratio of AC to core@shell were respectively 8 hours and 2. The effect of time on the antibacterial property of $Fe_3O_4@SiO_2/AC$ nanocomposite was then studied at the varying time (8, 16, and 24 hours) along with the selected values of temperature and ratio of AC to core@shell as 40 °C and 4, respectively. Also, the effect of various ratios of AC to core@shell was investigated in 2, 4, and 6, and the antibacterial property of $Fe_3O_4@SiO_2/AC$ nanocomposite was checked while the selected values of temperature and time were 40 °C and 24 hours, respectively.

McFarland 0.5 standard preparation method

The McFarland modulus is universally used in Antibiotic Susceptibility Test (AST) to standardize the assessment number of bacteria in a liquid substance suspension or broth culture of the bacterial cell by the divergence of the turbidity of the cultured test suspension with that of the McFarland Standard. A 0.5 McFarland standard was accumulated by mixing 0.5 mL of 1.175% (w/v) barium chloride dihydrate ($BaCl_2.2H_2O$)—with 9.95 mL of 1% (v/v) sulfuric acid (H_2SO_4). Mixing the two combinations forms a barium sulfate precipitate, which causes darkness in the solution. The resulting 0.5 McFarland suspension has an optical absorption of 0.08-0.13 at 625 nm. This turbidity was equivalent to approximately 1.8×10^8 (cfu/mL).

Revival of microbial strains

Bacteria must be activated 24 hours prior to preparation for microbial cultures after which the multiplication method was used. To study bacterial strains the following procedure is pursued every bacterium: The bacterium was harvested with a sterile swab from a standard bacterial medium next to the flame and on the disinfected workbench. Then, the impregnated swab was contacted on a plate, on which the name of the microbes has been previously labeled, in parallel lines in three orientations (vertical, horizontal, diagonal) so that the entire surface of the plate is covered by a single layer of the bacterium. Finally, the plates were incubated for 24 hours.

Preparation of different dilutions of $Fe_3O_4@SiO_2/AC$ nanocomposite

3000 µg/mL fresh stock $Fe_3O_4@SiO_2/AC$ nanocomposite solution was prepared in sterile dimethylsulfoxide (DMSO) solution. The fresh working solutions of $Fe_3O_4@SiO_2/AC$ nanocomposite with concentrations of 1000, 500, 250, 125, 62, 31.25, 62.15, 7.81, and 3.90 µg/mL were prepared appropriately diluted 9 times.

Provision of positive and negative controls

A concentration of 1000 µg/mL of imipenem was applied as a positive control for gram-negative and gram-positive bacteria. Also, 100 µL of DMSO as a negative control was added to each well.

Evaluation of Minimal Inhibitory Concentration (MIC) by dilution in liquid medium technique (Broth microdilution)

First, 3000 µg/mL of $Fe_3O_4@SiO_2/AC$ nanocomposite was prepared in DMSO solvent. Then, the stock solution was diluted 9 times (in serial 2-fold dilutions) and solutions with 1000, 500, 250, 125, 62, 31.25, 15.62, 7.81 and 3.90 µg/mL concentrations were obtained. To develop the microbial suspension, first, microbial strains were subcultured in sterile Mueller-Hinton Broth (MHB) and incubated to a turbidity of 0.5 McFarland standard, then were diluted in the ratio 1:150 to reach the final number of 1.5×10^8 cfu/mL Based on the number of bacterial strains, a 96-well microplate, arranged in 8 rows with 12 columns, containing broth medium and microbial agents at serial concentrations was set up for each bacterium. The wells of each row were numbered from 1 to 12. The value of 100 µL of 1000 µg/mL nanocomposite was added in well 1. Then 100 µL of microbial suspension was added to wells 2-12. In the following, 100 µL nanocomposite of different concentrations was added to the rest of numbered wells. Finally, the inoculated tubes were covered and incubated at the temperature of 37 °C for 24 hours. After incubation, the tubes were surveyed for turbidity caused by inoculated bacterial growth. The 2, 3, 5-triphenyl-tetrazolium
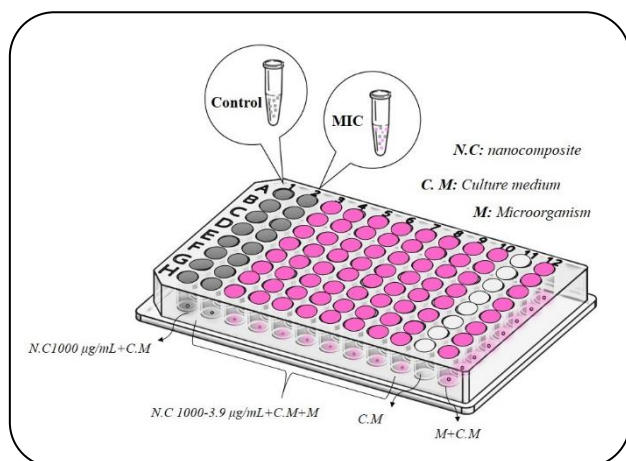
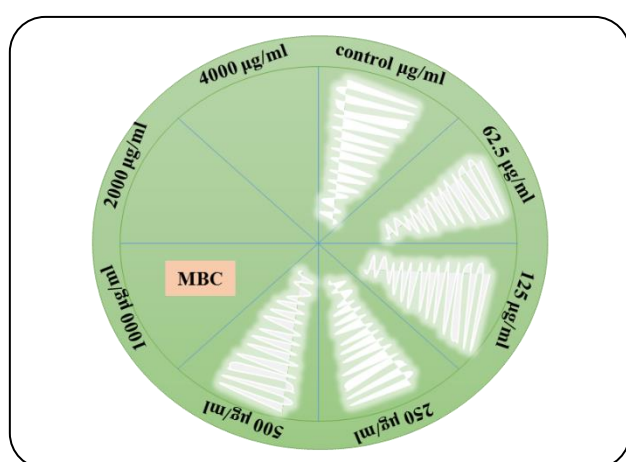**Fig. 1: 96-well plate image of a culture sample of S.epidermidis.**

Fig. 2: MBC plate image of cultured S.epidermidis bacteria.

chloride salt was used as a visual indicator for wells showing pink-colored microbial growth. MIC values were defined as the lowest concentration of $Fe_3O_4@SiO_2/AC$ nanocomposite that inhibited visible growth (Fig. 1)

Investigation of Minimal Bactericidal Concentration (MBC)

MBC has been defined as the minimum concentration of an antibiotic capable of killing 99% of the bacteria. To determine the Minimal Lethal Concentration (MBC) of $Fe_3O_4@SiO_2/AC$ nanocomposite, 50 µL volumes of all tubes in which no growth was observed were removed and streaked onto the Muller Hinton agar plate. Then inoculated media were incubated at the temperature of 37 °C for 24 hours. A house of the plate containing the lowest concentration of $Fe_3O_4@SiO_2/AC$ nanocomposite in which no bacterial growth was observed was considered as MBC (Fig. 2).

RESULTS AND DISCUSSION
Characterization of Magnetic Nano Particles (MNPs)

XRD patterns of the Fe_3O_4 and $Fe_3O_4@SiO_2$ nanoparticles and $Fe_3O_4@SiO_2/AC$ nanocomposite are shown in Fig. 3. All the reflection peaks for bare MNPs (Fig. 3a) were determined in 2θ = 30.1, 35.5, 43.3, 53.4, 57.0, and 62.5 assigned to 220, 311, 400, 422, 511, and 440 planes which are well-indexed to the inverse cubic spinel structure of Fe_3O_4 (JCPDS card no. 19–0629) according to the reflection peak positions and relative intensities [30, 31]. The same peaks were also observed in both XRD patterns of $Fe_3O_4@SiO_2$ (Fig. 3b) and $Fe_3O_4@SiO_2/AC$ (Fig. 3c). Additional peaks that existed at 20°- 30° can be attributed to the existence of amorphous SiO_2 in core@shell [32] and the activated carbon, respectively. The two activated carbon and magnetite peaks overlapped at $2\theta = 43.1\%$ with the formation of $Fe_3O_4@SiO_2/AC$ nanocomposites. This phenomenon leads to a reduction in the intensity of activated carbon diffraction. For this reason, this pattern is not recognizable by the naked eyes but it exists in the structure and the pattern can be justified by diffraction at $2\theta = 26.4°$ [33]. The mean size of nanocrystals was calculated using the Debye- Scherrer equation.

$$D = \frac{K\,\lambda}{\beta\cos\theta} \tag{2}$$

To compute the crystallite size of the MNPs and coated MNPs (D), the wavelength (λ) of the employed X-ray light and Debye-Scherrer permanent (K) were set to 0.54 nm and 0.94, respectively. K is also a constant that depends on the morphology of the crystals, which in this study is considered to be 0.94 due to the close proximity of the Fe_3O_4 particles to the spherical state. The peak width at mid-peak height (β) of the fracture angle was also used to conjecture the MNPs and coated MNPs particle scope and θ is the Bragg diffraction angle. The crystallite size of the prepared Fe_3O_4, $Fe_3O_4@SiO_2$, and $Fe_3O_4@SiO_2/AC$ were about 32.26, 37.10, and 46.3 nm, respectively. The difference in the size of Fe_3O_4, and $Fe_3O_4@SiO_2$ nanoparticles confirms the presence of the silica layer.

The SEM, EDAX, and TEM analysis

In Fig. 4, the SEM images of the $Fe_3O_4@SiO_2$, AC, and $Fe_3O_4@SiO_2/AC$, and TEM image of $Fe_3O_4@SiO_2/AC$ nanocomposite are shown. The synthesized $Fe_3O_4@SiO_2$ nanoparticles have rather orderly images. The size of the

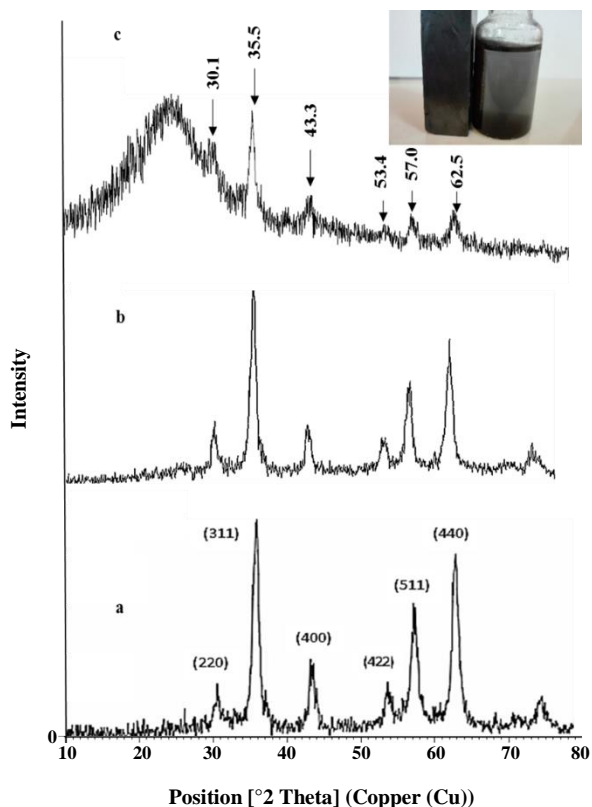***Fig. 3: X-ray diffraction patterns of nanoparticles a) Fe₃O₄, b) Fe₃O₄@SiO₂ and c) Fe₃O₄@SiO₂/AC.***

nanoparticles are evaluated to be in the range of 16-27 nm (Fig. 4a) approximately. Activated carbon produced from *Nigella sativa* oil waste showed relative cavities with the size of about 2-50 nm (Fig. 4b). The SEM image of Fe₃O₄@SiO₂/AC nanocomposite (Fig. 4c) shows the proper placement of produced core@shell nanoparticles in mesoporous cavities of activated carbon and the bond formation among them. TEM image nanocomposite (Fig. 4d) shows that core@shell nanospheres are uniformly distributed in the carbon active phase.

The corresponding EDAX spectrum (Fig. 5) and spot scanning images of Fe₃O₄@SiO₂ and Fe₃O₄@SiO₂/AC nanoparticles were obtained to assess their approximate chemical composition (Figs. **S1** and **S2**). The distribution of the elements (iron, oxygen, and silica) confirmed the formation of Fe₃O₄@SiO₂ magnetic nanoparticles. The quantitative results of spot scanning for the obtained nanoparticles were shown in Tables **S1** and **S2**. The results demonstrate that carbon atoms are the most abundant element in the Fe₃O₄@SiO₂/AC structure as a nanocomposite substrate with 74% weight percent.

BET characterization

According to the BET results, the size of the produced AC nanoporous from *Nigella sativa* oil waste was about 26 nm. Also, the high specific surface area of the AC indicates the resulting AC has the potential to be an appropriate substrate for bonding with Fe₃O₄@SiO₂ nanoparticles. The obtained results are given in Table 1. BET hysteresis isotherm of nanocomposite Fe₃O₄@SiO₂/AC represents in Fig. 6. In this isotherm model, according to the type of hysteresis ring can be determined that the shape and type of cavities. The hysteresis diagram shows the presence of mesopores in the material. According to the drawn hysteresis adsorption/ desorption diagram, it can be said that the cavities have a cylindrical shape that corresponds with type IV isotherms [34].

Investigation of the antibacterial effects

In this research, after characterization of the newly synthesized nanocomposite, it's potential as an antibacterial agent against two gram-positive bacteria *Staphylococcus* (1435: *S.epidermidis* PTCC) and *Streptococcus* (1768: *S.agalactiae* PTCC), and two gram-negative bacteria, *Calicilla* (1290: *K. pneumonia* PTCC) and *Salmonella* (1609: *S.typhi* PTCC) was investigated. Three parameters 1) formation temperature of nanocomposite (30, 40, 50 °C), 2) contact time of reaction (8, 16, 24 h), and 3) ratio of AC to Fe₃O₄@SiO₂ (2, 4, 6) supposed to effective factors on the antibacterial potential of the nanocomposite. The MIC and MBC amounts of the obtained samples are shown in Table 2 and Fig. **S3**. As can be seen from Table 2 and Fig. **S3** (a), the MIC and MBC values in temperatures 30 and 50° C for *Streptococcus* are 500 and 1000, respectively. Overly, it can be concluded that at these two temperatures, the nanocomposite has a greater effect on the bacteria *Streptococcus*. For economic reasons, we can consider temperature 30° C as the optimum temperature. As can be deduced from Table 2 and Fig. **S3** (b), MIC and MBC values of the nanocomposite did not change at different formation times for *Staphylococcus*, *Calicilla,* and *Salmonella* bacteria but the MBC value changed for *Streptococcus* bacterium at different formation times. The obtained results showed that MBC obtained 500 μg/mL for *Streptococcus* bacterium at a period of 24 h formation time. It can be concluded that synthesized nanocomposite was more effective in *Streptococcus* bacterium. Another point estimates of interest are that MBC values of the two examined gram-positive bacteria

Table 1: Results of BET analysis of activated carbon sample.

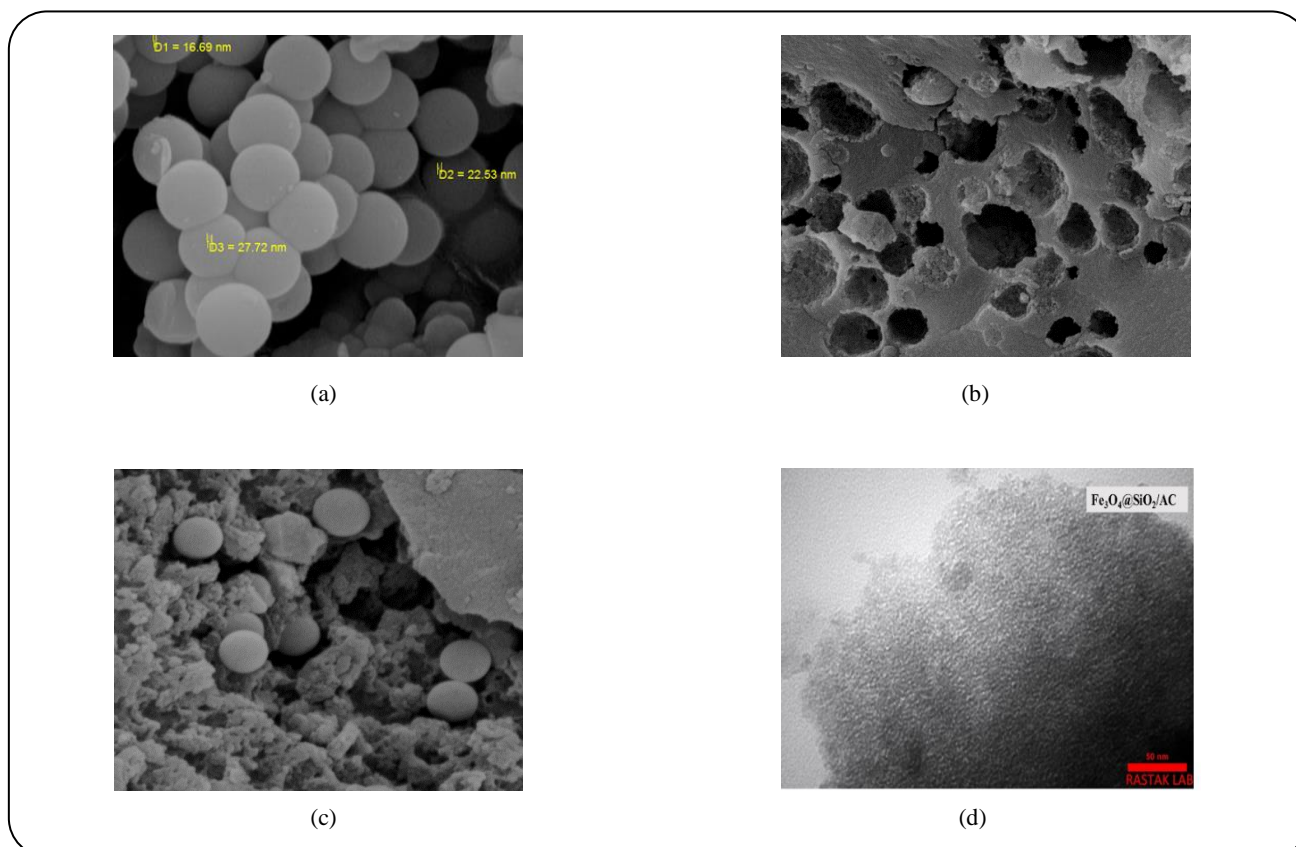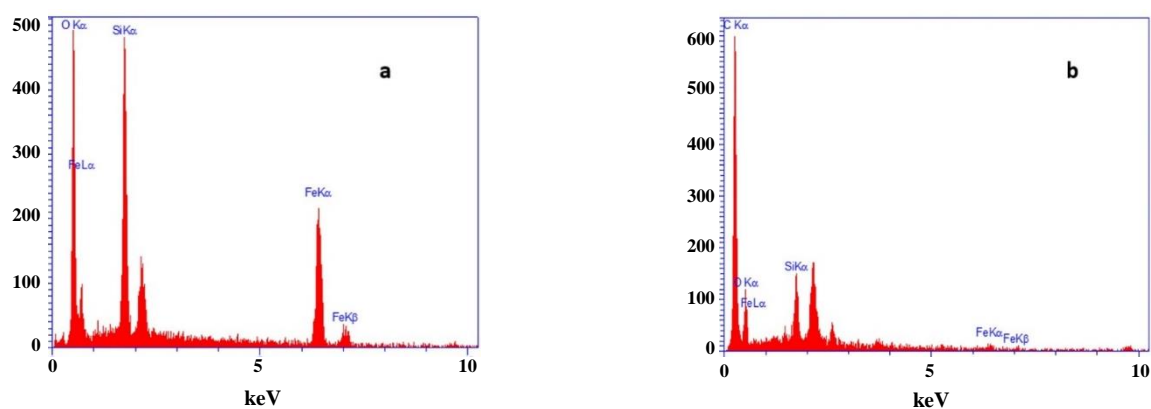| Physical properties	Volume
BET surface area (m^2/g)	112.23
Total volume (cm^2/g)	0.725
Median pore diameter (nm)	26.32

(a)

(b)

(c)

(d)

Fig. 4: SEM images of nanoparticles a) Fe₃O₄ @ SiO₂, b) Activated carbon (AC), c) Fe₃O₄@SiO₂/AC and d) TEM image of Fe₃O₄@SiO₂/AC.

Fig. 5: EDX diagrams of a) Fe₃O₄@SiO₂ and b) Fe₃O₄@SiO₂/AC.

Table 2: MIC and MBC values of prepared nanocomposites at different temperatures, times and ratios of AC to Fe₃O₄@SiO₂.

Parameters		S.epidermidis(Staphylococcus)		S.agalactiae (Streptococcus)		K.pneumonia(Calicilla)		S.typhi (Salmonella)	
		MBC [a]	MIC [b]	MBC	MIC	MBC	MIC	MBC	MIC
Temperature (^{0} C)	A: 30	1000	1000	1000	500	>1000	500	>1000	500
	B: 40	1000	1000	>1000	500	>1000	1000	>1000	500
	C: 50	1000	1000	1000	500	>1000	500	>1000	500
Time (h)	D: 8	1000	1000	>1000	500	>1000	500	>1000	500
	E: 16	1000	1000	1000	500	>1000	500	>1000	500
	F: 24	1000	1000	500	500	>1000	500	>1000	500
$\frac{AC}{Fe_3O_4@SiO_2}$	G: 2	1000	1000	>1000	500	>1000	500	>1000	500
	H: 4	1000	1000	1000	500	>1000	500	>1000	500
	I: 6	1000	1000	500	500	>1000	500	>1000	500
I.M.P (Imipenem)		128	64	32	4	>128	8	>128	64

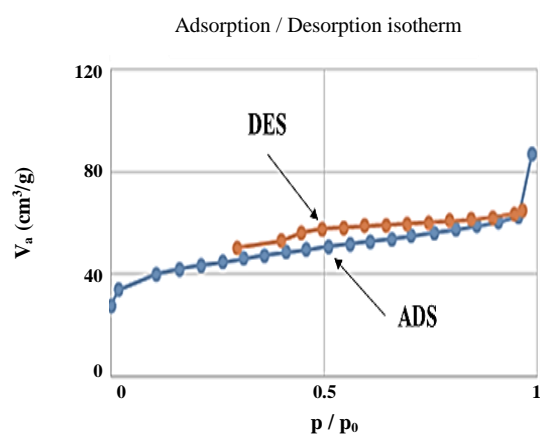[a & b] *Concentration unit is µg/ML*

Fig. 6: BET hysteresis isotherm of nanocomposite Fe₃O₄@SiO₂/AC.

are lower than the target gram-negative bacteria. This phenomenon could be attributed to the lack of outer membrane of positive bacteria which makes them more permeable to the external agents.

As shown in Table (2) and Fig. **S3 (c)**, the best MBC value against gram-positive *Streptococcus* bacterium was observed with AC to core@shell ratio equal to 6. The results also show that the effect of AC on the antimicrobial property of nanocomposite is greater when the ratio of AC to core@shell was raised from 2 to 6. For other bacteria, changes in AC to core@shell ratio did not affect the antimicrobial properties of the nanocomposite. In general,

the MBC values of gram-positive bacteria are still smaller than gram-negative bacteria. The low MBC for *Streptococcus* bacterium indicates that the prepared AC from the *Nigella sativa* is more attractive to gram-positive bacteria. This nanocomposite in optimal conditions, temperature= 30^0 C, contact time= 24 h, and AC to core@shell ratio = 6 has the best performance on gram-positive bacteria, especially *Streptococcus* bacteria. In this study, the Imipenem antibiotic was considered a positive control. MBC and MIC values of the Imipenem antibiotic compared to the studied bacteria are listed in Table 2 to compare the antibacterial properties of the produced nanocomposite with a strong antibiotic.

CONCLUSIONS

The magnetic nanoparticles of AC-Fe₃O₄ with combining Fe₃O₄@SiO₂ nanoparticles and activated carbon powder obtained from *Nigella sativa* oil waste were successfully synthesized and used as an inorganic antibacterial composite. The antibacterial performance of composite against some gram-positive and gram-negative bacteria was examined by considering influencing parameters including the temperature, time, and ratio of the activated carbon to Fe₃O₄@SiO₂. For this object, the MIC and MBC values of the prepared nanocomposites were investigated. The results show that time, temperature, and AC to core@shell ratio have effective roles in the properties of the synthesized nanocomposites. It was concluded that antibacterial

activities of the prepared nanocomposites enhanced with the temperature increase due to an increase in the penetration rate of core@shell into the AC cavities. Also, the nanocomposite formation becomes more uniform at higher temperatures. Regarding the operation times, it is observed that a higher core-shell contact time with AC increased the antibacterial activity. It seems that when nanocomposite is formed at longer times or as the ratio of AC to core@shell increases, the antimicrobial activity increases. The novel nanocomposite produced in this study is shown to have a positive and effective impact on gram-positive bacteria, especially *Streptococcus*. As a result, this magnetic nanocomposite possesses a high filtering activity against gram-positive bacteria. In addition, the presence of AC in the synthesized nanocomposite could make them a good absorbent for environmental and water contaminants.

REFERENCES

[1] Fekri M.H., Banimahd Keivani M., Darvishpour M., Banimahd Keivani H., Application of Electroactive Nano Composite Coated onto Wood Sawdust for the Removal of Malachite Green Dye from Textile Wastewaters, *J. Phys. Theor. Chem.*, **9(2)**: 95-102 (2012).

[2] Dashti Khavidaki H., Fekri M.H., Removing Thallium (I) Ion from Aqueous Solutions Using Modified ZnO Nanopowder, *J. Adv. Chem.*, **11(7)**: 3777-3788 (2015).

[3] Chegeni M., Khazaei A., Rahmati S., Fekri M.H., Perchloric Acid-Functionalized Silica Nanosphere as Novel and Green Catalyst for the Synthesis of 2H-Indazolo[2,1-b] Phthalazine-trione Derivatives, *Lett. Org. Chem.,* **12**: 471-477 (2015).

[4] Sohrabnezhad Sh., Jafarzadeh A., Antibacterial Activity of Mesoporous Silica Nanofibers, *Iran. J. Chem. Chem. Eng. (IJCCE),* **39(3)**: 1-11 (2020).

[5] Oroujzadeh N., New Chitosan-Silver Nanocomposites Containing N-NicontinylPhosphoric Triamide as an Antibacterial-Enhancer Additive. *Iran. J. Chem. Chem. Eng. (IJCCE),* **39(4)**: 1-9 (2020).

[6] Hajipour M.J., Fromm K.M., Ashkarran A.A., Aberasturi D.J.d., Larramendi I.R.d., Rojo T., Serpooshan V., Park W.J., Mahmoudi M., Antibacterial Properties of Nanoparticles. *Trends in Biotechnol.*, **30**: 499-511 (2012).

[7] Ghasemzadeh M.A., Abdollahi-Basir M.H., Babaei M., $Fe_3O_4@SiO_2–NH_2$ Core-shell Nanocomposite as an Efficient and Green Catalyst for the Ulticomponent Synthesis of Highly Substituted Chromeno [2, 3-b] Pyridines in Aqueous Ethanol Media, *Green. Chem. Let. Rev.,* **8**: 40-49 (2015).

[8] Prabhu Y.T., Venkateswara Rao K., Siva Kumari B., Kumar V.S.S., Pavani T., Synthesis of Fe_3O_4 Nanoparticles and its Antibacterial Application, *Int. Nano. Lett.*, **5**: 85-92 (2015).

[9] Heydari R., Foroutan Koudehi M., Pourmortazavi S.M., Antibacterial Activity of Fe_3O_4/Cu Nanocomposite: Green Synthesis Using Carum Carvi L. Seeds Aqueous Extract, *Chemistry Select*, **4**: 531-535 (2019).

[10] Qin Y., Zhang H., Tong Z., Song Z., Chen N., A Facile Synthesis of $Fe_3O_4@SiO_2@ZnO$ with Superior Photocatalytic Performance of 4-Nitrophenol, *J. Environ. Chem. Eng.*, **17**: 2207-2213 (2017).

[11] Jafari A., Farjami Shayesteh S., Salouti M., Boustani K., Effect of Annealing Temperature on Magnetic Phase Transition in Fe_3O_4 Nanoparticles, *J. Magn. Magn. Mater.*, **379**: 305-312 (2015).

[12] Lesnikovich A.I., Shunkevich T.M., Naumenko V.N., Vorobyova S.A., Baykov M.V., Dispersity of Magnetite in Magnetic Liquids and the Interaction with a Surfactant, *J. Magn. Magn. Mater.*, **85**: 14-16 (1990).

[13] Azgomi N., Mokhtary M., Nano-$Fe_3O_4@SiO_2$ Supported Ionic Liquid as an Efficient Catalyst for the Synthesis of 1, 3-Thiazolidin-4-ones under Solvent-free Conditions, *J. Mol. Catal. A: Chem.*, **398**: 58–64 (2015).

[14] Yang J., Qiu K., Preparation of Activated Carbons from Walnut Shells *via* Vacuum Chemical Activation and their Application for Methylene Blue Removal, *J. Chem. Eng.*, **165**: 209-217 (2010).

[15] Razavi Mehr M., Fekri M.H., Omidali F., Eftekhari N., Akbari-Adergani B., Removal of Chromium (VI) from Wastewater by Palm Kernel Shell-Based a Green Method, *J. Chem. Health Risks*, **9**(1): 75-86 (2019).

[16] Naeimi A., Honarmand M., Sedri A., Ultrasonic Assisted Fabrication of First MoO_3/Copper Complex Bio-nanocomposite Based on Sesbaniasesban Plant for Green Oxidation of Alcohols, *Ultrason. Sono Chem.*, **50**: 331-8 (2019).

[17] Hao Q., Liu Y., Chen T., Guo Q., Wei W., Ni B.J., Bi2O3@Carbon Nanocomposites for Solar-Driven Photocatalytic Degradation of Chlorophenols, *ACS Appl. Nano Mater.*, **2**, **4**: 2308-2316 (2019).

[18] Fekri M.H., Banimahd Keivani M., Razavi Mehr M., Akbari-Adergani B., Effective Parameters on Removal of Rhodamine B from Colored Wastewater by Nano Polyaniline/Sawdust Composite, *J. Mazandaran Univ. Med. Sci.*, **29(177)**: 166-179 (2019).

[19] Anjana P.M., Bindhub M.R., Umadevic M., Rakhia R.B., Antibacterial and Electrochemical Activities of Silver, Gold, and Palladium Nanoparticles Dispersed Amorphous Carbon Composites, *Appl. Surface Sci.*, **479**: 96–104 (2019).

[20] Kakavandi B., Jonidi Jafari A., Rezaei Kalantary R., Nasseri S., Ameri A., Esrafily A., Synthesis and Properties of Fe_3O_4-Activated Carbon Magnetic Nanoparticles for Removal of Aniline from Aqueous Solution: Equilibrium, Kinetic and Thermodynamic Studies, *Iran. J. Environ. Health Sci. Eng.*, **10**: 10-19 (2013).

[21] Yu Q., Fu A., Li H., Liu H., Lv R., Liu J., Guo P., Song Zhao X., Synthesis and Characterization of Magnetically Separable Ag Nanoparticles Decorated Mesoporous Fe_3O_4@Carbon with Antibacterial and Catalytic Properties, *Colloids and Surfaces A: Physicochem., Eng. Aspects*, **457**: 288–296 (2014).

[22] Furlan P.Y., Fisher A.J., Furlan A.Y., Melcer M.E., Shinn D.W., Warren J.B., Magnetically Recoverable and Reusable Antimicrobial Nanocomposite Based on Activated Carbon, Magnetite Nanoparticles, and Silver Nanoparticles for Water Disinfection, *Inventions*, **2**: 2-15 (2017).

[23] Kafilzade F., Behzadi Shahrbabak S., Isolation and Characterization Anthracene Degrading Gram-Negative Bacteria from the Contaminated Water and Sediment Contaminated in Maharlu Lake, *Environment. Sci. Technol*, **16**: 513-519 (2015).

[24] Te-Hsing W., Yi-Der T., Lie-Hang S., The Novel Methods for Preparing Antibacterial Fabric Compositescontaining Nano-Material, *Solid State Phenom.*, **124**: 1241-1244 (2007).

[25] Huh A.J., Kwon Y.J., Nanoantibiotics: A New Paradigm for Treatment Infectious Diseases Using Nanomaterials in the Antiobutics resistant Era, *J. Controlled Release*, **156**: 128–145 (2011).

[26] Thill A., Cytotoxicity of CeO_2 Nanoparticles for Escherichia Coli. Physico-Chemical Insight of the Cytotoxicity Mechanism, *Environ. Sci. Technol.*, **40**: 6151–6156 (2006).

[27] Ahmadi E., Abdollahi A., Najafipour S., Meshkibaf M.H., Fasihi-Ramandi M., Namdar N., Abdollahi S., Mousavi S.M., SamiZadeh B., Allahverdi G.H., Surveying the Effect of the Phenol Compounds on Antibacterial Activity of Herbal Extracts: *In vitro* Assessment of Herbal Extracts in Fasa-Fars Province, *J. Fasa Univ. Med. Sci.,* **6**: 210-220 (2016).

[28] Girginova P.L., Daniel-da-Silva A.L., Lopes C.B., Figueira P., Otero M., Amaral V.S., Pereira E., Trindade T.J., Silica Coated Magnetite Particles for Magnetic Removal of Hg^{2+} from Water, *Colloid Interface Sci.*, **345**: 234-240 (2010).

[29] Gupta A.K., Gupta M., Synthesis and Surface Engineering of Iron Oxide Nanoparticles for Biomedical Applications, *Biomaterials*, **26**: 3995-4021 (2005).

[30] Peng X., Wang Y., Tang X., Liu W., Functionalized Magnetic Core-Shell Fe_3O_4@SiO_2 Nanoparticles as Selectivity-Enhanced Chemosensor for Hg (II), *Dyes Pigm.*, **91**: 26-32 (2011).

[31] Duhan S., Devi S., Synthesis and Structural Characterization of Iron Oxide-Silica Nanocomposites Prepared by the Sol-Gel Method, *International J. Electronics Eng.*, **2**: 89-92 (2010).

[32] Hessien M.M., Rashad M.M., Zaky R.R., Abdel-Aal E.A., El-Barawy K.A., Controlling the Synthesis Conditions for Silica Nanosphere from Semi-Burned Rice Straw. *Materials Sci. Eng. B*, **162**: 14–21 (2009).

[33] Kakavandi B., Jahangiri-rad M., Rafiee M., Ramazanpour Effahani A., Babaei A.A., Development of Response Surface Methodology for Optimization of Phenol and p-Chlorophenol Adsorption on Magnetic Recoverable Carbon, *Micro Meso Mat.*, **231**:192-206 (2016).

[34] Rouquerol F., Rouquerol J., Llewellyn P., Sing K.S.W., Maurin G., "Adsorption by Powders and Porous Solids", 2nd ed., Elsevier (2013).